was spun at 60 rpm. Slower rotation speeds combined with higher average deposition rates (0.174 mmol h^{-1}) convert the starting material directly to colloid. It was essential in this case to maintain metal atom deposition conditions comparable to those used in the microscale experiments. Note that only a maximum 1.2% conversion of the starting material is expected under the macropreparative conditions.

Mo atoms (0.025 mmol) were deposited at 2.5 kV and 40 mA at 4.5 × 10^{-6} Torr. The green fluid was transferred cold under Ar backpressure to a Schlenk tube maintained at 77 K. An electronic absorption spectrum was obtained by anaerobic cold transfer of an aliquot of fluid to the 180 K quartz optical window of a cryostat.[3] Figure 6 (bottom) shows the electronic absorption spectrum of the starting bis(α,α,α-trifluorotoluene)molybdenum

complex exhibiting absorption maxima at 315 (MLCT) and 395 nm. The middle spectrum for the product of this reaction indicates a new absorption at 420 nm adjacent to the absorption of the starting organometallic target molecule. This band probably owes its origin to a species containing two molybdenum atoms in analogy to the product arising from a similar reaction between Dow Corning 510 fluid and molybdenum atoms.[13]

Contribution from The Heyrovsky Institute of Physical Chemistry and Electrochemistry, Dolejskova 3, 182 23 Prague 8, Czechoslovakia, and Department of Chemistry and Biochemistry, University of Colorado, Boulder, Colorado 80309-0215

Oxidative Substitution of Mn(CO)$_5^-$ by 3,5-Di-*tert*-butyl-1,2-benzoquinone. Synthesis and Characterization of the Unsaturated Mn(CO)$_3$(DBCat)$^-$ Anion

František Hartl,[†] Antonín Vlček, Jr.,*,[†] Lynn A. deLearie,[‡] and Cortlandt G. Pierpont*,[‡]

Bu$_4$N$^+$ and PPN$^+$ salts of the Mn(CO)$_3$(DBCat)$^-$ anion were prepared by oxidative substitution of two CO ligands of Mn(CO)$_5^-$ by 3,5-di-*tert*-butyl-1,2-benzoquinone. The product was characterized by crystallography and by UV–vis, IR, ^{13}C, and ^{1}H NMR spectroscopy. The complex exhibits some unusual properties: (i) it is a five-coordinate, formally 16-electron, species that shows no tendency to add a sixth ligand, (ii) π-acceptor (CO) and π-donor (catecholate) ligands are combined in the coordination sphere, and (iii) intense LMCT absorption bands are observed. Strong Cat → Mn π donation seems to account for this behavior. The complex exhibits two one-electron ligand-localized oxidations at –0.03 and +0.86 V (vs Ag/AgCl) and a one-electron reduction at –1.72 V. The primary product of the first oxidation, Mn(CO)$_3$(DBSQ), readily coordinates with a donor solvent molecule. Crystals of Bu$_4$N$^+$[Mn(CO)$_3$(DBCat)] form in the triclinic space group $P\bar{1}$ in a unit cell of dimensions a = 10.462 (2) Å, b = 21.629 (4) Å, c = 24.915 (9) Å, α = 102.61 (2)°, β = 93.19 (2)°, γ = 96.87 (2)°, and V = 5443 (2) Å^3. Three crystallographically independent formula units are contained within the asymmetric region of the unit cell. None of the three independent Mn(CO)$_3$(DBCat)$^-$ anions have regular coordination geometries, but one has a structure that is close to trigonal bipyramidal, while the other two anions have structures that are closer to a square-pyramidal geometry.

Introduction

The photochemical addition of *o*- and *p*-benzoquinones to Mn$_2$(CO)$_{10}$ has been studied extensively.[1–11] Reaction appears to proceed by addition of the quinone to the photogenerated Mn(CO)$_5$ radical. One-electron oxidative addition gives the six-coordinate semiquinone Mn(I) species Mn(SQ)(CO)$_5$. Oxidation of the metal destabilizes bonding to the carbonyl ligands. When *o*-quinones are used in these reactions, further CO dissociation concomitant with semiquinone chelation leads to the coordinatively saturated Mn(SQ)(CO)$_4$ species. However, these complexes remain susceptible to photochemical CO displacement to give Mn(SQ)$_2$ complexes upon irradiation in the presence of additional *o*-benzoquinone.[4] Catecholate ligands are more effective π donors than the *o*-semiquinones, and there is evidence that chelated catecholate ligands may, synergistically, stabilize the bonding to π acceptors.[12] To investigate this possibility, we have examined the reaction between 3,5-di-*tert*-butyl-1,2-benzoquinone and the Mn(CO)$_5^-$ anion. This reaction might be expected to occur by way of a two-electron oxidative addition process to give the chelated catecholate anion Mn(DBCat)(CO)$_4^-$, with stabilized CO coordination by virtue of catechol π donation. Rather, we have found that the product is the coordinatively unsaturated five-coordinate complex Mn(DBCat)(CO)$_3^-$, formed by further carbonyl displacement. In this report we present details on the synthesis and characterization of the complex.

Results

Formation and Characterization of Mn(CO)$_3$(DBCat)$^-$. The light yellow color of the CH$_2$Cl$_2$ solution of Mn(CO)$_5^-$ immediately turns deep red upon addition of 1 (or less) molar equiv of DBQ.[13] The reaction proceeds without the formation of long-lived intermediates. The 1:1 stoichiometry of the reaction

(1) Bowmaker, G. A.; Campbell, G. K. *Aust. J. Chem.* **1979**, *32*, 1897–1904.
(2) Alberti, A.; Camaggi, C. M. *J. Organomet. Chem.* **1979**, *181*, 355–363.
(3) Foster, T.; Chen, K. S.; Wan, J. K. S. *J. Organomet. Chem.* **1980**, *184*, 113–124.
(4) Lynch, M. W.; Hendrickson, D. N.; Fitzgerald, B. J.; Pierpont, C. G. *J. Am. Chem. Soc.* **1981**, *103*, 3961–3963.
(5) Tumanskij, B. L.; Sarbasov, K.; Solodovnikov, S. P.; Budnov, N. N.; Prokofev, A. I.; Kabachnik, M. I. *Dokl. Akad. Nauk SSSR, Ser. Khim.* **1981**, *259*, 611–616.
(6) Sarbasov, K.; Tumanskij, B. L.; Solodovnikov, S. P.; Bubnov, N. N.; Prokofev, A. I.; Kabachnik, M. I. *Izv. Akad. Nauk SSSR, Ser. Khim.* **1982**, 550–555.
(7) Abakumov, G. A.; Cherkasov, V. K.; Shalnova, K. G.; Teplova, I. A.; Razuvaev, G. A. *J. Organomet. Chem.* **1982**, *236*, 333–341.
(8) Vlcek, A., Jr. *J. Organomet. Chem.* **1986**, *306*, 63–75.
(9) Vlcek, A., Jr. *Photochemistry and Photophysics of Coordination Compounds*; Yersin, H., Vogler, A., Eds.; Springer-Verlag: Berlin, Heidelberg, 1987; pp 267–270.
(10) Kaim, W. *Coord. Chem. Rev.* **1987**, *76*, 187–235.
(11) Wang, S. R.; Cheng, C. P.; Ho, I.-I. *J. Chem. Soc., Dalton Trans.* **1988**, 2695–2699.
(12) Shorthill, W. B.; Buchanan, R. M.; Pierpont, C. G.; Ghedini, M.; Dolcetti, G. *Inorg. Chem.* **1980**, *19*, 1803–1805.
(13) Abbreviations used for quinone: DBQ = 3,5-*tert*-butyl-1,2-benzoquinone, PQ = 9,10-phenanthrenequinone, CQ = tetrachloro-1,2-benzoquinone. The corresponding catecholate dianions: DBCat, PCat, CCat. Semiquinone radical anions: DBSQ, PSQ, CSQ.

[†] The Heyrovsky Institute of Physical Chemistry and Electrochemistry.
[‡] University of Colorado.

was confirmed electrochemically by the titration of the THF solution of electrochemically generated $Mn(CO)_5^-$ with a THF solution of DBQ. The anodic wave of $Mn(CO)_5^-$, observed polarographically, disappeared completely after the addition of exactly 1 molar equiv of DBQ with concomitant formation of waves corresponding to the reaction product (vide infra). Outer-sphere electron transfer between $Mn(CO)_5^-$ and DBQ appears not to take place, as the reaction mixture is EPR silent and no evidence for the formation of either $Mn_2(CO)_{10}$, free DBSQ, or free DBCat was found by polarography or by IR spectroscopy.

The product of the reaction between $Mn(CO)_5^-$ and DBQ was isolated as PPN^+ and Bu_4N^+ salts. The presence of three intense $\nu(CO)$ vibrations at 1990, 1886, and 1870 cm^{-1} for the PPN^+ salt (Nujol) points to the presence of three CO ligands bound to Mn(I) in a low-symmetry coordination geometry. The IR spectrum of the Bu_4N^+ salt in Nujol is more complex, consisting of two high-frequency bands at 2005 and 1998 cm^{-1}, of a band at 1891 cm^{-1} with an unresolved shoulder on its high-energy side, and of a band at 1880 cm^{-1}. In CH_2Cl_2 solution this compound exhibits only two bands at 1998 and 1891 (broad) cm^{-1}. The only IR evidence for the presence of the DBCat ligand is bands at 1419 and 1298 cm^{-1} (Bu_4N^+) or at 1412 and 1302 cm^{-1} (PPN^+). Other ligand IR bands are obscured by those of the cations.

The presence of the DBCat ligand can be clearly seen from both ^1H and ^{13}C NMR spectroscopy. The ^1H NMR spectrum obtained in CD_2Cl_2 exhibits two signals at 1.48 and 1.24 ppm belonging to *tert*-butyl groups bound at C_3 and C_5 positions of the catecholate ring,[13] respectively. The resonances of the C_4- and C_6-bound protons occur as doublets centered at 6.90 and 6.59 ppm, $J(H,H)$ = 2.1 Hz. Proton resonances of the PPN^+ cation were observed as a strong, unresolved peak at 7.47 ppm. Integration indicated one DBCat ligand for each PPN^+ cation. ^1H NMR spectroscopy also indicated the presence of benzene molecules of crystallization for both salts of the complex. Integration indicated a 2:1 benzene to complex anion ratio for the PPN^+ salt, while for the Bu_4N^+ salt the molar ratio of benzene to complex was approximately 0.17. The presence of weakly bound benzene molecules in solid samples of the two salts was further confirmed by mass spectroscopy.

The ^{13}C NMR spectra exhibit resonances both of the DBCat carbons and the carbon atoms of the CO ligands. Integration of the ^{13}C NMR peaks was performed carefully by using inverse gated decoupling to suppress NOE. The following peaks were found (number of C atoms and assignment[13] are given in parentheses): δ 30.0 ppm (3 C, CH_3 of C_5-Bu^t), 32.3 (3 C, CH_3 of C_3-Bu^t), 34.3 (1 C, C_5-Bu^t), 35.0 (1 C, C_3-Bu^t), 109.6 (1 C, C_6), 110.3 (1 C, C_4), 126.8 and 127.9 (6 C, PPN^+, ^{31}P coupling), 128.6 (12 C, C_6H_6), 130.3 (12 C, PPN^+), 132.6 (12 C, PPN^+), 133.8 (1 C, C_3), 134.7 (6 C, PPN^+), 137.6 (1 C, C_5), 158.5 (1 C, C_2), 161.5 (1 C, C_1), 229.9 (3 C, CO). The observation of only a single CO resonance at 229.9 ppm ($\Delta\nu_{1/2}$ = 28.1 Hz) is in accord with the expected fluxionality of the $Mn(CO)_3$ unit.

The integral values of the ^{13}C NMR peaks clearly point to the composition: three CO ligands per DBCat with one PPN^+ and two benzene solvate molecules. The sharp appearance of the spectrum and the absence of extraordinary chemical shifts verify the diamagnetism of the complex, consistent with a Mn(I)–DBCat charge distribution.

The IR, ^1H NMR, and ^{13}C NMR data and elemental analyses show that the reaction products are $PPN[Mn(CO)_3(DBCat)]\cdot 2C_6H_6$ and $Bu_4N[Mn(CO)_3(DBCat)]\cdot^1/_6C_6H_6$. It may be concluded that $Mn(CO)_5^-$ reacts with DBQ by a two-electron oxidative substitution (eq 1). This reaction is the two-electron

$$Mn(CO)_5^- + DBQ \rightarrow Mn(CO)_3(DBCat)^- + 2CO \quad (1)$$
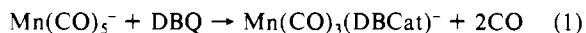
analogue of the one-electron oxidative substitution that takes place between the $Mn(CO)_5$ radical and DBQ during the photolysis of $Mn_2(CO)_{10}$ in the presence of DBQ.[3,5,7–9]

The reactions of two other quinones, 9,10-phenanthrenequinone (PQ) and *o*-chloranil (CQ), with $Mn(CO)_5^-$ have also been studied in THF or CH_2Cl_2 solutions. Both appear to react differently from DBQ, possibly by more than a single reaction pathway. The dominant reaction of CQ is a slow electron-transfer process that
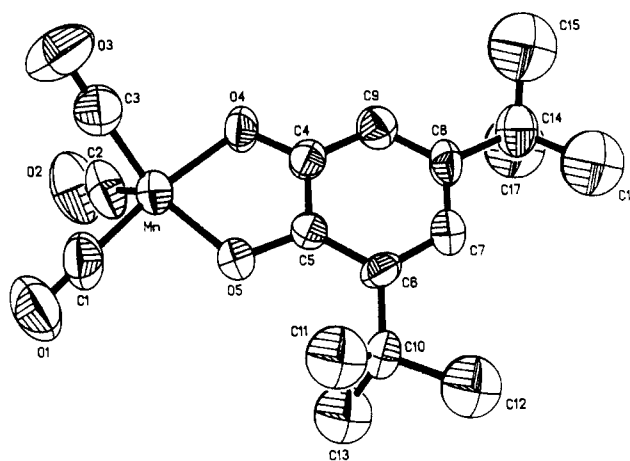
Figure 1. View of the $Mn(CO)_3(DBCat)^-$ anion that most closely resembles a trigonal bipyramid in structure. The trans C1–Mn–O4 angle is 170.4 (3)°, and angles within the equatorial plane are 87.2 (5), 135.0 (4), and 137.8 (4).

gives $Mn_2(CO)_{10}$, as observed by solution IR spectroscopy. Reduction of CQ apparently occurs to give the catecholate, as the reaction is EPR silent. A transient complex with $\nu(CO)$ overlapping with the 1901-cm^{-1} band of unreacted $Mn(CO)_5^-$ was observed, and $Mn(CO)_5Cl$ is formed as one of the reaction products.

In the case of PQ, slow electron transfer gives $Mn_2(CO)_{10}$ (IR) and PSQ (EPR), but this is not the main pathway. An additional reaction produces an unidentified product that shows strong absorptions at 581 and 442 nm and no $\nu(CO)$ bands. It appears to be a Mn complex with PSQ or PCat ligands.

Although the reactions of $Mn(CO)_5^-$ with CQ and PQ were not studied in detail, it is obvious that strong donation by DBCat together with the moderate oxidizing potential of DBQ contributes to the relative simplicity of reaction 1. Similar differences among DBQ, PQ, and CQ have been observed for the one-electron oxidative addition to $Co(CN)_5^{3-}$ [14] and to other metal–carbonyl complexes.[15]

Structural Characterization of $Bu_4N[Mn(CO)_3(DBCat)]\cdot^1/_6C_6H_6$. The complicated IR spectrum and unusual solvent stoichiometry of the Bu_4N^+ salt of $Mn(CO)_3(DBCat)^-$, relative to its PPN^+ salt, stimulated interest in the solid-state structure. Since the metal centers of $Mn(CO)_3(DBCat)^-$ are coordinatively unsaturated, there is the additional possibility for a bridged structure with catecholate oxygen atoms of adjacent complex anions occupying the sixth coordination sites of the d^6 metals.[16]

The crystal structure of $Bu_4N[Mn(CO)_3(DBCat)]$ consists of three independent cations and anions and a benzene solvate molecule located about a crystallographic inversion center. Selected bond distances and angles are given in Table I. The three independent Mn centers are all five-coordinate. All three have coordination geometries that are intermediate between trigonal bipyramidal and square pyramidal; one is closer to TBP (Mn), and the other two are closer to SP (Mn′, Mn″). The TBP geometry about Mn, shown in Figure 1, contains catecholate oxygen O4 and carbonyl carbon C1 in axial sites and atoms C2, C3, and O4 in equatorial sites. The trans axial angle is 170.4 (3)°, and the equatorial angles are 87.2 (5), 135.0 (4), and 137.8 (4)°, with the contracted angle between the equatorial carbonyl ligands. In this structure the catecholate ligand occupies axial and equatorial sites, while for the two SP molecules shown in Figures 2 and 3 the catecholate chelates to basal sites, with carbonyl carbon atoms C1′ and C1″ occupying axial positions. Basal trans angles to Mn′ are 154.4 (4) and 166.5 (4)° to the catecholate oxygens, and to

(14) Vlcek, A., Jr.; Klima, J.; Vlcek, A. A. *Inorg. Chim. Acta* **1983**, *69*, 191–197.

(15) Lynch, M. W.; Buchanan, R. M.; Pierpont, C. G.; Hendrickson, D. N. *Inorg. Chem.* **1981**, *20*, 1038–1047.

(16) For example: Buchanan, R. M.; Pierpont, C. G. *Inorg. Chem.* **1979**, *18*, 1616–1620.

Table I. Selected Bond Distances (Å) and Angles (deg) for Bu₄N[Mn(CO)₃(DBCat)]

Manganese Coordination

Mn–O4	1.962 (6)	Mn′–O4′	1.929 (6)	Mn″–O4″	1.925 (6)
Mn–O5	1.896 (5)	Mn′–O5′	1.903 (5)	Mn″–O5″	1.901 (6)
Mn–C1	1.782 (12)	Mn′–C1′	1.727 (11)	Mn″–C1″	1.707 (14)
Mn–C2	1.726 (12)	Mn′–C2′	1.774 (11)	Mn″–C2″	1.739 (13)
Mn–C3	1.736 (10)	Mn′–C3′	1.735 (8)	Mn″–C3″	1.769 (14)
O5–Mn–O4	82.6 (2)	O5′–Mn′–O4′	82.1 (2)	O5″–Mn″–O4″	82.9 (3)
C1–Mn–O4	170.4 (3)	C1′–Mn′–O4′	104.1 (4)	C1″–Mn″–O4″	103.8 (5)
C1–Mn–O5	88.3 (3)	C1′–Mn′–O5′	117.9 (3)	C1″–Mn″–O5″	119.6 (4)
C2–Mn–O4	98.0 (4)	C2′–Mn′–O4′	166.5 (4)	C2″–Mn″–O4″	93.5 (5)
C2–Mn–O5	135.0 (4)	C2′–Mn′–O5′	91.0 (3)	C2″–Mn″–O5″	151.2 (5)
C2–Mn–C1	90.7 (5)	C2′–Mn′–C1′	89.5 (5)	C2″–Mn″–C1″	89.0 (6)
C3–Mn–O4	94.0 (4)	C3′–Mn′–O4′	91.9 (4)	C3″–Mn″–O4″	166.3 (5)
C3–Mn–O5	137.8 (4)	C3′–Mn′–O5′	154.4 (4)	C3″–Mn″–O5″	87.9 (5)
C3–Mn–C1	90.6 (5)	C3′–Mn′–C1′	87.7 (4)	C3″–Mn″–C1″	89.5 (6)
C3–Mn–C2	87.2 (5)	C3′–Mn′–C2′	89.4 (4)	C3″–Mn″–C2″	89.7 (6)

Carbonyl Ligands

O1–C1	1.139 (14)	O1′–C1′	1.165 (13)	O1″–C1″	1.170 (18)
O2–C2	1.188 (14)	O2′–C2′	1.164 (13)	O2″–C2″	1.154 (16)
O3–C3	1.163 (13)	O3′–C3′	1.193 (10)	O3″–C3″	1.148 (19)
O1–C1–Mn	178.0 (9)	O1′–C1′–Mn′	177.9 (8)	O1″–C1″–Mn″	178.4 (13)
O2–C2–Mn	179.6 (7)	O2′–C2′–Mn′	174.4 (9)	O2″–C2″–Mn″	178.6 (13)
O3–C3–Mn	177.1 (9)	O3′–C3′–Mn′	178.1 (9)	O3″–C3″–Mn″	176.1 (12)

Catecholate Ligands

O4–C4	1.343 (9)	O4′–C4′	1.334 (9)	O4″–C4″	1.344 (11)
O5–C5	1.352 (11)	O5′–C5′	1.335 (10)	O5″–C5″	1.343 (11)
C4–C5	1.400 (12)	C4′–C5′	1.384 (12)	C4″–C5″	1.390 (13)
C5–C6	1.401 (11)	C5′–C6′	1.401 (11)	C5″–C6″	1.396 (14)
C6–C7	1.370 (14)	C6′–C7′	1.400 (12)	C6″–C7″	1.388 (13)
C7–C8	1.376 (13)	C7′–C8′	1.379 (11)	C7″–C8″	1.392 (12)
C8–C9	1.374 (11)	C8′–C9′	1.401 (11)	C8″–C9″	1.369 (12)
C4–C9	1.398 (14)	C4′–C9′	1.379 (12)	C4″–C9″	1.394 (13)
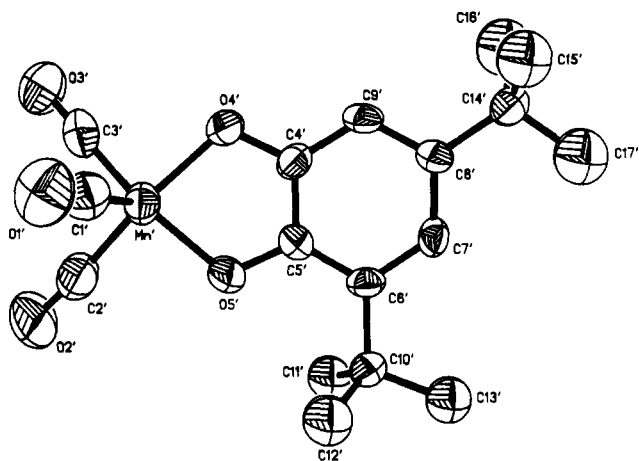
Figure 2. View of the primed Mn(CO)₃(DBCat)⁻ anion. The coordination geometry most closely resembles a square pyramid, with the catecholate ligand chelated in the basal plane and the carbonyl ligand containing C1′ bonded in the apical position.

Figure 3. View of the double-primed Mn(CO)₃(DBCat)⁻ anion. As in the case of the primed molecule, the coordination geometry resembles a square pyramid, with the carbonyl ligand containing C1″ bonded at the apical site.

Mn″ the angles are 151.2 (5) and 166.3 (5)°. Examination of the Mn–O and Mn–C lengths in Table I shows that the carbonyl ligands bonded directly trans to catecholate oxygen atoms with trans angles exceeding 165° have the longest Mn–C lengths of the structure and that the catecholate oxygen atoms bonded trans to these carbonyl ligands have the longest Mn–O lengths. It is of interest that the coordinatively saturated, six-coordinate Mn-(CO)₄(DBCat)⁻ species, which likely forms as a precursor to Mn(CO)₃(DBCat)⁻, would have two CO ligands directly trans to catecholate oxygen atoms and two trans to one another. Since the strong donation of the catecholate ligand appears to destabilize the trans CO ligands and trans CO ligands are known to destabilize one another, displacement of the fourth carbonyl ligand would apparently lead to net stabilization of bonding to both the CO and DBCat ligands of Mn(CO)₃(DBCat)⁻.

Features of the three independent DBCat ligands agree with values found in other structure determinations. The average C–O

length of 1.342 (9) Å is exactly the value expected for a catecholate and different from values of 1.29 and 1.24 Å expected for semiquinone and benzoquinone ligands.[17]

Electronic Absorption Spectra. Two intense bands are observed for Mn(CO)₃(DBCat)⁻ at 436 nm (ϵ = 6250 L mol⁻¹ cm⁻¹) and 548 nm (ϵ = 8300) in THF solution. These band positions are virtually solvent independent with the following absorption maxima found in other solvents: CH₂Cl₂, 542, 438 nm; DMF, 549, 438 nm; benzene, 546, 435 nm. On the basis of their high extinction coefficients, both bands are assigned as LMCT (DBCat → Mn) transitions. However, the absence of solvatochromism points[18] to a transition between highly delocalized orbitals, which might

(17) Pierpont, C. G.; Buchanan, R. M. *Coord. Chem. Rev.* **1981**, *38*, 45–87.
(18) Balk, R. W.; Snoeck, T.; Stufkens, D. J.; Oskam, A. *Inorg. Chem.* **1980**, *19*, 3015–3021.

result from a high degree of mixing between manganese and catecholate orbitals. Moreover, the identity of absorption spectra in coordinating and noncoordinating solvents shows that the $Mn(CO)_3(DBCat)^-$ complex does not behave as a Lewis acid.

Chemical and Electrochemical Properties. In THF, the complex $Mn(CO)_3(DBCat)^-$ exhibits two one-electron oxidations at -0.03 and $+0.86$ V and a one-electron reduction at -1.72 V (vs Ag/AgCl). The reduction is both electrochemically and chemically reversible ($i_c/i_a = 1.0$ at a scan rate of 20 mV/s). As no reducible ligands are present, the reduction has to be localized at the metal to give the 17-electron radical $Mn^0(CO)_3(DBCat)^{2-}$.

Both oxidations are electrochemically quasireversible. The first oxidation is chemically reversible ($i_a/i_c = 1$), producing the semiquinone complex $Mn(CO)_3(DBSQ)$, which rapidly coordinates a THF molecule to form $Mn(CO)_3(THF)(DBSQ)$, as judged from the characteristic EPR signal ($g = 2.0042$, $A_{Mn} = A_H = 0.37$ mT)[7,8] obtained by in situ electrolysis. The second oxidation is apparently also localized at the ligand, producing a quinone complex $Mn(CO)_3(THF)(DBQ)^+$, which is chemically unstable ($i_a/i_c = 0.75$ at 100 mV/s).

The most prominent chemical properties of $Mn(CO)_3(DBCat)^-$ are a lack of Lewis acidity and its oxidation reactions. As indicated by the visible absorption spectra, the complex does not coordinate weak bases like THF or DMF. Stronger basis (pyridine, PPh_3) cause more complicated substitutions that were not studied further. Several oxidizing agents (O_2, DBQ, I_2, $FeCp_2BF_4$) react with the complex in THF to produce a mixture of radical products including DBSQ and $Mn(CO)_3(DBSQ)(THF)$. Both chemical and electrochemical oxidations are currently under investigation in order to compare their products with those of controlled photolysis of $Mn_2(CO)_{10}$ with *o*-DBQ.

Discussion

Structure and Bonding in $Mn(CO)_3(DBCat)^-$. The catecholate ligands are well-known to be strong σ and π donors, stabilizing high metal oxidation states, particularly for the second- and third-row metals.[19] It is of interest that, in $Mn(CO)_3(DBCat)^-$, catecholate coordination is to a low-valent metal, Mn(I). This situation has been described previously in four-coordinate complexes of Rh(I) and Ir(I),[12,20] but it occurs much less commonly for first-row metals. Despite being a five-coordinate, formally 16-electron species, the complex shows little tendency to add a sixth ligand to achieve an 18-electron configuration. Transfer of additional charge to the metal through π donation appears to provide compensation for the missing sixth ligand, and in a rigorous sense, it is probably not proper to view the metal as a 16-electron center. Ligand-based oxidation to give $Mn(CO)_3(DBSQ)$ dramatically increases the acidity of the metal, and the complex readily adds additional ligands including ethers, phosphines, phosphites, and amines.[2,6-8] This change in the character of the metal upon ligand oxidation is a clear consequence of the decrease in the π-donation property of semiquinone relative to catecholate.

These bonding features can be understood by using the qualitative MO diagram shown in Scheme I. In this treatment the $Mn(CO)_3(DBCat)^-$ anion is assumed to have C_s symmetry, with the plane of symmetry intersecting the catecholate ligand. *tert*-Butyl substituents have been neglected. The (A) and (S) symbols denote orbital symmetry with respect to the mirror plane, and the bonding scheme is analogous to that used in the bonding discussion for isoelectronic (triphos)Co(DBCat)$^+$.[21] Three filled orbitals of the C_{3v} $Mn(CO)_3^+$ fragment, $1a_1 + 1e$, are used for π back-bonding to the CO ligands.[21-23] All three empty $2a_1 + 2e$ orbitals of $Mn(CO)_3^+$ interact strongly with the catecholate.

Scheme I
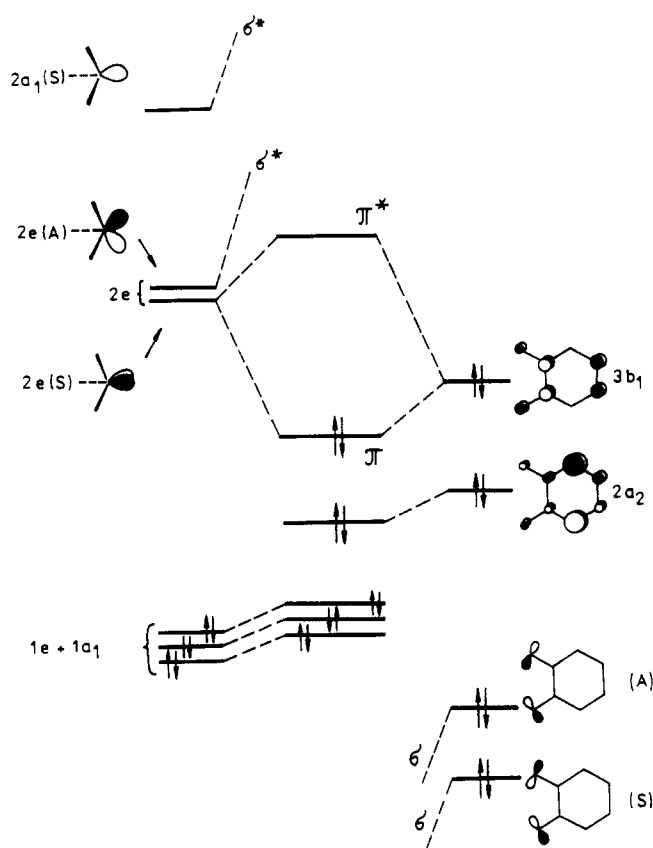
Table II. Crystallographic Data for $Bu_4N[Mn(CO)_3(DBCat)]\cdot^1/_6C_6H_6$

chem formula	$MnC_{34}H_{57}NO_5$	space group	$P\bar{1}$ (No. 2)
fw	614.9	T	296 °C
a	10.462 (2) Å	λ	0.71069 Å
b	21.629 (4) Å	ρ_{obsd}	1.14 g·cm^{-3}
c	24.915 (9) Å	ρ_{calcd}	1.11 g·cm^{-3}
α	102.61 (2)°	μ	3.58 cm^{-1}
β	93.19 (2)°	transm coeff	0.902–0.975
γ	96.87 (2)°	$R(F_o)$	0.067
V	5443 Å^3	$R_w(F_o)$	0.081
Z	6		

Two, $2a_1(S) + 2e(A)$, are responsible for σ bonding, whereas the $2e(S)$, which is mainly 3d + 4p in character, interacts strongly with the $3b_1(S)$ HOMO of the catecholate. The π delocalization has a stabilizing effect, and admixture of the $2e(S)$ orbital into the π HOMO of the complex increases charge on the metal above its formal 16-electron configuration. In turn, the energy of the $1a_1 + 1e$ set raises and Mn $\rightarrow$ CO back-donation increases. Due to the complete involvement of the $2a_1 + 2e$ set in Mn–DBCat bonding, $Mn(CO)_3(DBCat)^-$ is stable and exhibits no Lewis acidity.

Upon oxidation to $Mn(CO)_3(DBSQ)$, the π orbital becomes partially occupied. This, together with stabilization of the $3b_1$ orbital, leads to a considerable decrease in π bonding within the Mn–O–C–C–O ring. The $2e(S)$ orbital becomes almost non-bonding and available for σ donation with a Lewis base. Other aspects of the redox chemistry of $Mn(CO)_3(DBCat)^-$ are also in accord with this MO scheme.

The observed lack of solvatochromism is experimental evidence for π delocalization within the catecholate chelate ring. Also, the catecholate C–O lengths are comparable to the values found for catecholate complexes of high oxidation state metals where π donation is clearly a factor. The increase in charge on the metal is reflected in the low values for the ν(CO) frequencies, which are much lower than those found in six-coordinate complexes containing the $Mn(CO)_3^+$ fragment (e.g.: $CpMn(CO)_3$, 2025 and 1938 cm^{-1}; $Mn(CO)_3L_3$ (L = py), 2041, 1947 cm^{-1}; $Mn(CO)_3L_3$

(19) (a) deLearie, L. A.; Haltiwanger, R. C.; Pierpont, C. G. *Inorg. Chem.* **1987**, *26*, 817–821. (b) deLearie, L. A.; Pierpont, C. G. *Inorg. Chem.* **1988**, *27*, 3842–3845.
(20) Girgis, A. Y.; Sohn, Y. S.; Balch, A. L. *Inorg. Chem.* **1975**, *14*, 2327–2331.
(21) Bianchini, C.; Masi, D.; Mealli, C.; Meli, A.; Martini, G.; Laschi, F.; Zanello, P. *Inorg. Chem.* **1987**, *26*, 3683–3693.
(22) Hoffmann, R.; Elian, M. *Inorg. Chem.* **1975**, *14*, 1058–1076.
(23) Albright, T. S.; Burdett, J. K.; Whangbo, M.-H. *Orbital Interactions in Chemistry*; Wiley Interscience: New York, 1985; pp 381–387.

Table III. Atomic Coordinates ($\times 10^4$) and Derived Isotropic Displacement Parameters ($\times 10^3$, $\mathring{A}^2$) for Bu₄N[Mn(CO)₃(DBCat)]·¹/₆C₆H₆

	x/a	y/b	z/c	$U(eq)^a$		x/a	y/b	z/c	$U(eq)^a$
Mn	4734 (1)	1918 (1)	6806 (1)	54 (1)	C12'	4756 (9)	2817 (4)	10986 (4)	75 (3)ᶜ
Mn'	2010 (1)	1110 (1)	9683 (1)	51 (1)	C13'	4649 (9)	3910 (4)	10876 (3)	68 (3)ᶜ
Mn''	713 (2)	-3132 (1)	6364 (1)	71 (1)	C14'	-279 (8)	3819 (4)	10472 (3)	55 (4)
O1	6767 (8)	1247 (3)	7166 (3)	108 (4)	C15'	-1297 (9)	3625 (5)	10850 (4)	86 (3)ᶜ
O2	5075 (9)	1376 (4)	5653 (3)	123 (5)	C16'	-1013 (10)	3846 (5)	9932 (4)	106 (4)ᶜ
O3	2788 (8)	836 (4)	6778 (3)	124 (4)	C17'	363 (10)	4479 (5)	10743 (4)	94 (3)ᶜ
O4	3464 (5)	2481 (3)	6684 (2)	59 (2)	C18'	4258 (9)	2835 (4)	5393 (4)	67 (4)
O5	5501 (5)	2656 (3)	7336 (2)	54 (2)	C19'	5034 (10)	3478 (5)	5591 (5)	91 (5)
O1'	1272 (7)	242 (3)	10380 (3)	94 (4)	C20'	6229 (10)	3421 (5)	5959 (5)	101 (6)
O2'	4297 (7)	457 (3)	9476 (3)	114 (4)	C21'	6947 (13)	4043 (6)	6243 (5)	146 (5)ᶜ
O3'	646 (7)	175 (3)	8733 (3)	86 (3)	C22'	3302 (10)	2995 (4)	4493 (4)	71 (4)
O4'	649 (5)	1642 (3)	9720 (2)	50 (2)	C23'	4166 (9)	2622 (5)	4125 (4)	75 (5)
O5'	3022 (5)	1903 (2)	10029 (2)	51 (2)	C24'	4227 (10)	2874 (5)	3604 (4)	95 (6)
O1''	1814 (12)	-3305 (5)	7397 (4)	170 (6)	C25'	4947 (11)	2513 (5)	3182 (5)	122 (4)ᶜ
O2''	-1033 (11)	-4301 (4)	6264 (5)	174 (6)	C26'	2400 (9)	2098 (5)	4895 (4)	65 (4)
O3''	2602 (12)	-3842 (5)	5773 (5)	219 (8)	C27'	1825 (9)	1863 (4)	5357 (3)	64 (4)
O4''	-590 (5)	-2592 (3)	6581 (2)	58 (3)	C28'	1456 (10)	1140 (4)	5188 (4)	76 (5)
O5''	1407 (6)	-2434 (3)	6071 (2)	64 (3)	C29'	702 (10)	875 (5)	5601 (4)	99 (4)ᶜ
N	1190 (7)	2449 (3)	8259 (3)	47 (3)	C30'	2146 (9)	3233 (4)	5337 (3)	66 (4)
N'	3033 (7)	2788 (3)	5023 (3)	52 (3)	C31'	841 (10)	3205 (5)	5044 (4)	87 (5)
N''	-318 (7)	-1871 (3)	8334 (3)	56 (3)	C32'	-23 (11)	3608 (5)	5402 (5)	105 (6)
C1	5958 (11)	1499 (5)	7026 (4)	76 (5)	C33'	271 (13)	4290 (6)	5414 (5)	139 (5)ᶜ
C2	4934 (10)	1595 (5)	6124 (5)	82 (5)	C1''	1383 (14)	-3231 (5)	6975 (6)	110 (7)
C3	3573 (11)	1264 (5)	6775 (5)	71 (5)	C2''	-336 (15)	-3833 (6)	6311 (6)	117 (7)
C4	3740 (9)	3052 (4)	7013 (3)	48 (4)	C3''	1841 (14)	-3581 (5)	6011 (5)	114 (7)
C5	4852 (8)	3167 (4)	7379 (3)	44 (4)	C4''	-333 (9)	-2016 (4)	6460 (3)	47 (4)
C6	5232 (8)	3762 (4)	7742 (3)	50 (4)	C5''	758 (9)	-1928 (4)	6177 (3)	48 (4)
C7	4467 (9)	4229 (4)	7719 (4)	56 (4)	C6''	1121 (8)	-1347 (5)	6032 (3)	52 (4)
C8	3377 (10)	4140 (4)	7361 (4)	55 (4)	C7''	381 (8)	-860 (4)	6201 (3)	49 (4)
C9	3008 (9)	3551 (4)	7012 (3)	56 (4)	C8''	-697 (8)	-934 (4)	6496 (3)	46 (4)
C10	6444 (9)	3866 (4)	8142 (4)	63 (4)	C9''	-1058 (8)	-1516 (4)	6615 (3)	45 (4)
C11	6418 (10)	3376 (5)	8498 (4)	93 (3)ᶜ	C10''	2292 (9)	-1260 (4)	5688 (4)	66 (4)
C12	6608 (10)	4523 (5)	8530 (4)	104 (4)ᶜ	C11''	2127 (10)	-1762 (5)	5156 (4)	89 (3)ᶜ
C13	7608 (10)	3828 (5)	7817 (4)	100 (4)ᶜ	C12''	2486 (10)	-601 (5)	5548 (4)	88 (3)ᶜ
C14	2610 (10)	4693 (4)	7328 (4)	74 (5)	C13''	3519 (10)	-1323 (5)	6024 (4)	97 (4)ᶜ
C15	1184 (13)	4505 (7)	7308 (6)	164 (6)ᶜ	C14''	-1467 (10)	-369 (4)	6684 (4)	68 (4)
C16	2904 (12)	5268 (6)	7806 (5)	135 (5)ᶜ	C15''	-2221 (22)	-214 (9)	6159 (7)	79 (7)ᶜ
C17	2870 (13)	4939 (6)	6831 (5)	142 (5)ᶜ	C15''ᵇ	-1501 (38)	45 (16)	6267 (13)	91 (12)ᶜ
C18	2172 (8)	2074 (4)	8482 (4)	62 (4)	C16''	-2451 (21)	-476 (9)	7109 (10)	85 (7)ᶜ
C19	3495 (9)	2169 (5)	8300 (4)	82 (5)	C16''ᵇ	-704 (28)	45 (15)	7235 (15)	89 (12)ᶜ
C20	4342 (9)	1724 (5)	8510 (4)	84 (5)	C17''	-495 (17)	272 (9)	6973 (9)	84 (7)ᶜ
C21	3997 (10)	1034 (5)	8241 (4)	101 (4)ᶜ	C17''ᵇ	-2908 (29)	-613 (12)	6837 (14)	63 (10)ᶜ
C22	954 (8)	2215 (4)	7641 (3)	57 (4)	C18''	298 (9)	-1537 (4)	8910 (3)	64 (4)
C23	-85 (9)	2488 (4)	7361 (3)	66 (4)	C19''	1529 (8)	-1754 (4)	9087 (3)	61 (4)
C24	-219 (9)	2200 (5)	6747 (4)	85 (5)	C20''	2133 (10)	-1313 (5)	9644 (4)	93 (5)
C25	-1221 (10)	2481 (5)	6448 (4)	103 (4)ᶜ	C21''	3211 (12)	-1570 (6)	9872 (5)	126 (4)ᶜ
C26	-48 (8)	2337 (5)	8535 (3)	64 (4)	C22''	-1380 (9)	-1506 (4)	8188 (3)	63 (4)
C27	-717 (9)	1660 (4)	8400 (4)	67 (4)	C23''	-2546 (9)	-1520 (5)	8535 (4)	74 (5)
C28	-1909 (9)	1605 (5)	8710 (4)	82 (5)	C24''	-3433 (10)	-1063 (5)	8405 (4)	95 (6)
C29	-2505 (10)	899 (5)	8619 (4)	104 (4)ᶜ	C25''	-4539 (11)	-1023 (5)	8747 (5)	119 (4)ᶜ
C30	1656 (8)	3154 (4)	8380 (3)	58 (4)	C26''	-820 (9)	-2551 (4)	8341 (4)	65 (4)
C31	2164 (9)	3479 (4)	8963 (4)	69 (4)	C27''	-1649 (10)	-2935 (4)	7833 (4)	73 (5)
C32	2503 (10)	4177 (5)	9015 (4)	86 (5)	C28''	-1958 (11)	-3611 (5)	7863 (4)	99 (6)
C33	3181 (11)	4549 (5)	9544 (4)	107 (4)ᶜ	C29''	-2965 (12)	-3988 (6)	7432 (5)	137 (5)ᶜ
C1'	1554 (9)	585 (5)	10091 (4)	61 (4)	C30	659 (9)	-1868 (4)	7906 (3)	62 (4)
C2'	3426 (10)	743 (4)	9554 (4)	72 (5)	C31'	1369 (9)	-1221 (4)	7893 (4)	70 (5)
C3'	1187 (9)	553 (4)	9126 (4)	59 (4)	C32''	2534 (10)	-1303 (5)	7555 (4)	83 (5)
C4'	1037 (8)	2246 (4)	9990 (3)	41 (4)	C33''	3221 (11)	-664 (5)	7532 (5)	120 (4)ᶜ
C5'	2344 (8)	2393 (4)	10155 (3)	41 (4)	C34ᵇ	5782	4851	4567	180
C6'	2839 (7)	3021 (4)	10426 (3)	41 (4)	C35ᵇ	4442	4768	4461	180
C7'	1969 (8)	3469 (3)	10524 (3)	38 (3)	C36ᵇ	3660	4918	4894	180
C8'	663 (8)	3329 (4)	10364 (3)	42 (4)	C37ᵇ	6294	5021	4887	180
C9'	199 (8)	2697 (4)	10092 (3)	42 (3)	C38ᵇ	5319	4800	4459	180
C10'	4311 (8)	3210 (4)	10591 (3)	48 (4)	C39ᵇ	4025	4778	4572	180
C11'	5023 (8)	3076 (4)	10066 (3)	61 (3)ᶜ					

ᵃ Equivalent isotropic U defined as one-third of the trace of the orthogonalized U_{ij} tensor. ᵇ See Experimental Section for details on refinement of disordered carbon atoms. ᶜ Atoms refined with isotropic thermal parameters.

(L = CH₃CN), 2063, 1974 cm⁻¹; Mn(CO)₃L₃ (L = acetone), 2020, 1931 cm⁻¹).[24,25] Carbonyl stretching frequencies reported for the 17-electron Mn(CO)₃L₂ radicals (L = phosphine, phosphite) are lower in the 1890–1850-cm⁻¹ range.[26]

The only other five-coordinate Mn(I) complex that has, to our knowledge, been structurally characterized is Mn(CO)₃(2,2,6,6-tetramethylpiperidinyl-1-oxyl).[27,28] The nitroxyl ligand is π

(24) Nakamoto, K. *Infrared and Raman Spectra of Inorganic and Coordination Compounds*, 4th ed.; Wiley Interscience: New York, 1986.

(25) Drew, D.; Darensbourg, D. J.; Darensbourg, M. Y. *Inorg. Chem.* **1975**, *14*, 1579–1584.

(26) McCullen, S. B.; Brown, T. L. *J. Am. Chem. Soc.* **1982**, *104*, 7496–7500.

bonded to the metal to form a Mn–N–O metallacycle. It is a much weaker π donor than the catecholate, as shown by the higher values of the $\nu(CO)$ frequencies (2031, 1933, 1915 cm^{-1}). Another five-coordinate, formally 16-electron, Mn(I) complex has been detected by EPR spectroscopy, Mn(CO)$_3$(Bu^t-DAB$^-$) (Bu^t-DAB = Bu^{t}N–CH–CH–NBu^t).[29] The DAB$^-$ ligand donates one π electron in the manner of a semiquinone, and the complex, as well as its Re analogue, resembles the isoelectronic Mn(CO)$_3$(DBSQ) complex in electronic structure.

Conclusions

1. Mn(CO)$_5^-$ undergoes two-electron oxidative substitution of two carbonyl ligands by DBQ to give the formally 16-electron complex Mn(CO)$_3$(DBCat)$^-$.

2. The five-coordinate, coordinatively unsaturated complex anion contains a low-valent metal chelated by the strongly π-donating DBCat ligand. Donation by the DBCat ligand results in strong LMCT bands in the visible spectrum and in the low lewis acidic character of the metal.

3. The π-donor character of DBCat is lost upon oxidation to DBSQ, and in consequence, Mn(CO)$_3$(DBSQ) readily adds donor solvent molecules and other Lewis bases as sixth ligands.

Experimental Section

Materials. Mn$_2$(CO)$_{10}$ (Strem) was vacuum-sublimed. DBQ (Aldrich) was recrystallized from heptane, whereas PQ (Fluka), CQ (Fluka), (PPN)Cl (Aldrich), and Bu$_4$NCl (Aldrich) were used as received. Solvents were carefully purified by standard procedures and deoxygenated either by a ketyl method (THF) or by degassing with pure argon.

General Procedures. All synthetic procedures were carried out on a Schlenk line under an atmosphere of argon. The UV–vis, IR, and EPR solution cells were filled under argon by using gastight syringes. Samples for NMR analysis were prepared in 5-mm tubes sealed on the vacuum line. Nujol mulls for IR spectra were prepared in an argon-filled glovebag by using vacuum-degassed Nujol.

Infrared spectra were recorded on Perkin-Elmer 257, 684, and 1710 (FTIR) spectrometers. ^{1}H and ^{13}C NMR spectra were recorded on a Bruker AM400, and a Varian XL200 was used for some ^{1}H NMR spectra. The detailed assignment of individual resonances was based on special pulsing and two-dimensional NMR techniques (APT, long-range INEPT, HETCOR) and on empirical δ estimates using additivity constants. A JEOL JMS-D100 was used to obtain mass spectra. UV–vis absorption spectra were measured with a Carl Zeiss (Jena) M-40 spectrophotometer. X-Band EPR spectra were recorded on a Varian E-4 with DPPH used as the g value standard. Both polarographic and cyclic voltammetric experiments were performed with an LP-4 instrument on a DME, an HMDE, or a Pt electrode. An aqueous Ag/AgCl (10^{-1} M LiCl) reference electrode and Pt-wire auxiliary electrodes were used. The $E_{1/2}$ of the Fc$^+$/Fc couple was found at +0.64 V. Preparative electrolysis of Mn$_2$(CO)$_{10}$ was used to prepare solutions containing known concentrations of Mn(CO)$_5^-$. Procedures were carried out in a three-compartment cell by using a Hg-pool working electrode under polarographic control. Bu$_4$NPF$_6$ (10^{-1} M) electrolyte was used in all electrochemical experiments.

Syntheses. PPN[Mn(CO)$_5$] was prepared by modification of a published procedure.[30] Sodium–potassium alloy was used to reduce Mn$_2$-(CO)$_{10}$ instead of Na–amalgam.[31] Reduction by NaK alloy proceeds completely without byproducts, and the resulting solution can be easily filtered.

PPN[Mn(CO)$_3$(DBCat)]·2C$_6$H$_6$. A 149-mg (0.7-mmol) sample of DBQ dissolved in 4 mL of CH$_2$Cl$_2$ was added dropwise to a vigorously

stirred solution containing 483 mg (0.7 mmol) of PPN[Mn(CO)$_5$] in 4 mL of CH$_2$Cl$_2$. The color immediately turned deep wine red. After the solution was stirred for 15 min, 10 mL of degassed benzene was added. CH$_2$Cl$_2$ was distilled off under vacuum, and the volume of the solution was reduced to 5 mL. The microcrystalline product that separated from the solution was filtered out and washed several times with cold deoxygenated benzene. The product, characterized as PPN[Mn(CO)$_3$-(DBCat)], was obtained in 70% yield based on PPN[Mn(CO)$_5$].

Bu$_4$N[Mn(CO)$_3$(DBCat)]·^{1}/$_6$C$_6$H$_6$. A 975-mg (2.5-mmol) sample of Mn$_2$(CO)$_{10}$ was reduced with NaK alloy in 1:1 THF/isooctane to give a solution of Bu$_4$N[Mn(CO)$_5$] by following the procedure for the preparation of the PPN$^+$ salt. Addition of a stoichiometric equivalent of DBQ gave the product characterized as Bu$_4$N[Mn(CO)$_3$(DBCat)]·^{1}/$_6$C$_6$H$_6$ by using the procedure described above. Crystals suitable for X-ray analysis were grown by the addition of benzene to a saturated CH$_2$Cl$_2$ solution of the complex.

Both PPN$^+$ and Bu$_4$N$^+$ salts of Mn(CO)$_3$(DBCat)$^-$ are dark red solids that are oxidized by air within a few minutes. Solutions of the complex are extremely air sensitive and may undergo oxidation by excess DBQ. Consequently, excess DBQ in the synthesis should be avoided.

C, H, and N elemental analyses were consistent with the compositions of Bu$_4$N[Mn(CO)$_3$(DBCat)] and PPN[Mn(CO)$_3$(DBCat)]. Apparently, the benzene solvate molecules were lost during sample heating prior to the analysis. The presence of solvate in crystalline samples has been confirmed by X-ray diffraction (Bu$_4$N$^+$) and by NMR spectroscopy (PPN$^+$).

Structure Determination of Bu$_4$N[Mn(CO)$_3$(DBCat)]. A crystal of the complex was mounted on a glass fiber, coated with an amorphous resin, and the fiber was aligned on a Nicolet P3/F automated diffractometer. Axial photographs indicated only triclinic symmetry for the crystal. Unit cell dimensions given in Table II were calculated from the centered positions of 25 reflections with 2θ values between 20 and 25°. Additional parameters and details of procedures used for data collection, structure determination, and refinement are contained in the supplementary material.

The unit cell volume, together with the experimental crystal density, indicated that there were three independent sets of Bu$_4$N$^+$ cations and Mn(CO)$_3$(DBCat)$^-$ anions per unit cell. One *tert*-butyl group of the DBCat ligand bonded to the double-primed complex anion, atoms C15'' to C17'', was found to be disordered. Methyl carbon atoms of this group were refined in two sets of positions with half-occupancy factors. Upon covergence of preliminary cycles of refinement, the benzene solvate molecule was located on a difference Fourier map about the inversion center at (^{1}/$_2$, ^{1}/$_2$, ^{1}/$_2$). Electron density in this region resembled a torus. The benzene solvate was included in the refinement as a rigid group defined by six quarter carbon atoms, atoms C34 to C39, located in the asymmetric region about the inversion center. Final cycles of least-squares refinement converged with discrepancy indices of $R = 0.067$ and $R_w = 0.081$. Final positional and isotropic thermal parameters for all non-hydrogen atoms are listed in Table III. A stereoview of the asymmetric region of the unit cell and tables containing anisotropic thermal parameters, hydrogen atom locations and thermal parameters, and structure factors are available as supplementary material.

Supplementary Material Available: A stereoview showing the contents of one asymmetric region of the unit cell of Bu$_4$N[Mn(CO)$_3$-(DBCat)]·^{1}/$_6$C$_6$H$_6$ and tables giving crystal data and details of the structure determination, anisotropic thermal parameters, and hydrogen atom locations (15 pages); a listing of observed and calculated structure factors (22 pages). Ordering information is given on any current masthead page.

(27) Jaitner, P.; Huber, W.; Huttner, G.; Scheidsteger, O. *J. Organomet. Chem.* **1983**, *259*, C1–C5.

(28) Rehder, D.; Jaitner, P. *J. Organomet. Chem.* **1987**, *329*, 337–342.

(29) Andrea, R. R.; deLange, W. G. J.; van der Graaf, T.; Rijkhoff, M.; Stufkens, D. J.; Oskam, A. *Organometallics* **1988**, *7*, 1100–1106.

(30) Faltynek, R. A.; Wrighton, M. S. *J. Am. Chem. Soc.* **1978**, *100*, 2701–2705.

(31) Ellis, J. E.; Flown, E. A. *J. Organomet. Chem.* **1975**, *99*, 263–268.